GENERATING A HIERARCHY OF REDUCED MODELS FOR A SYSTEM OF DIFFERENTIAL EQUATIONS MODELING THE SPREAD OF *WOLBACHIA* IN MOSQUITOES*

ZHUOLIN QU† AND JAMES M. HYMAN†

Abstract. We create and analyze a hierarchy of reduced order models for the spread of a *Wolbachia* bacteria infection in mosquitoes. Mosquitoes that are infected with some strains of the *Wolbachia* bacteria are much less effective at transmitting zoonotic diseases, including Zika, chikungunya, dengue fever, and other mosquito-borne diseases. The infection will persist in a wild mosquito population only if the fraction of infected mosquitoes exceeds a minimum threshold. Mathematical models can be used to understand the complex maternal transmission of *Wolbachia* infection and to guide efforts for keeping the infection above the threshold. This threshold can be characterized as a backward bifurcation for a system of nine ordinary differential equations modeling the *Wolbachia* infection in a heterosexual mosquito population. Although this system captures the detailed transmission dynamics, they are difficult to analyze. We describe the mathematical approach used in each model reduction to create a system of seven, four, or two ordinary differential equations that capture the important properties of the original system. We evaluate the quality of the approximation at each step by comparing the associated important dimensionless numbers, analyzing the critical threshold condition for each reduced model, and using phase plane analysis to demonstrate that all the reduced models accurately reproduce the dynamics of the full system.

Key words. mosquito-borne diseases, model reduction, backward bifurcation, mathematical modeling, sensitivity analysis

AMS subject classifications. 92D30, 34K18, 93A30

1. Introduction.

Mosquito-borne diseases are often controlled by reducing the population size of mosquitoes by spraying insecticide, larval control, and biological control such as the sterile insect technique. These approaches require a sustained mitigation program to maintain effectiveness. Recently, instead of reducing the population of wild mosquitoes, scientists have been infecting them with *Wolbachia* bacteria to reduce their ability to transmit zoonotic diseases to humans. *Wolbachia* interferes with the replication of arboviruses, including dengue fever [10], chikungunya [10], Zika [3, 1], and yellow fever [15], and greatly reduces the ability of mosquitoes to spread these infections [18].

Wolbachia is a natural parasitic microbe found in about 60% of wild insect species [4], including mosquitoes. However, it is rarely found in the *Aedes aegypti* (*A. aegypti*) that spread these arboviruses. Since *Wolbachia* is not naturally abundant in the *A. aegypti* population, this implies that if a small number of these mosquitoes are infected, then the infection dies out. That is, *Wolbachia* infection has a basic reproductive number less than one in a population of wild mosquitoes.

Mathematical models and recent large-scale field releases of infected mosquitoes have demonstrated that, even though a small infection will die out, if the fraction of infected mosquitoes exceeds a threshold, then a *Wolbachia* epidemic can be sustained in mosquitoes. This threshold can be understood as a backward bifurcation in the stability analysis of the mathematical models [19, 11].

For these models to accurately capture this threshold condition, they must account for the complex maternal transmission routes throughout a mosquito's lifecycle as well as the impact of fitness cost induced by *Wolbachia* infection. In [19], a two-

*Submitted to the editors DATE.

†Department of Mathematics, Tulane University, New Orleans, LA USA 70118 (zqu1@tulane.edu,mhyman@tulane.edu)

sex compartmental model of six ordinary differential equations (ODEs) was proposed to model different infection status in males, females, and aquatic-stage mosquitoes and take into account the fitness change as well as the cytoplasmic incompatibility between infected males and uninfected females.

In [11], this model was extended to a system of nine ODEs that includes multiple pregnant stages of females to distinguish the unmated females from the mated ones and treat the cytoplasmic incompatibility phenomenon explicitly as one of the three pregnant stages in the mated females. In [7], an even larger system (13 ODEs) that included each stage of the aquatic-stage mosquitoes (egg, larvae, pupae) was proposed, and the fitness cost from infection was modeled as a reduced egg-laying rate for infected females and reduced lifespans for both infected females and males.

These ODE models capture the transmission dynamics in each mosquito group, but they all assume that the infection is spatially homogeneous (uniform) in the mosquito populations. When infected mosquitoes are released in the wild, even though the ratio of infected mosquitoes can exceed the threshold in the center of the release region, it will be below the threshold at the edges of the release zone. The models must be extended to capture this spatial heterogeneity and temporal variations to analyze if the infected region will grow or shrink and collapse. This can be achieved by including the diffusion and transport of mosquitoes and extending the ODE models to a system of partial differential equations (PDEs) [20].

The difficulty of analyzing large systems of 9 or 13 PDEs have led some researchers to propose a system of 2 ODEs for the spread of *Wolbachia*. The 2 ODEs are then generalized to a manageable system of 2 nonlinear partial differential diffusion equations to account for the spatial heterogeneity. Unfortunately, the existing 2-ODE models have been based on heuristics so that the solution behaves in a physically realistic way, instead of being derived from the more detailed model. Also, the parameters in the simple model are not defined in terms of the biologically relevant parameters as used in the detailed ODE models, which makes it hard to estimate their values from the biological lab results [15].

We will derive the reduced models through a step-by-step analysis that allows all the parameters of the reduced models to be defined as explicit functions of the parameters for the full model. We first define the parameters for the complex 9-ODE model, which models the biologically relevant quantities. Next, we either identify

- variables that have the least impact on the quantities of interest or
- relationships between the variables that are constant, or slowly varying, for the parameters and initial conditions of interest.

We use this information to reduce the number of variables and differential equations being solved while preserving key quantities of interest for the model, such as the important dimensionless numbers for the system of equations. We then verify that the model reduction does not significantly alter the dynamics of the solution in the regions of interest.

We start by recognizing that the aquatic stage plays a minor role in the maternal transmission cycle. We eliminate the aquatic stage to create a 7-ODE model where the parameters are functions of the 9-ODE model. The death, delay, and carrying capacity of aquatic stages [11] are accounted for by modifying the birth rates and death rates in the 7-ODE model (subsection 3.1). Moreover, female mosquitoes quickly become pregnant after hatching. This biologically realistic assumption allows us to assume that the fraction of single females is relatively small and combine single and pregnant females into a single variable and reduce the 7-ODE model to a 4-ODE model (subsection 3.2). Finally, we identify a nonlinear proportional relationship

between the infection prevalence in male and female mosquito populations in the full model solutions. We use this relationship to define the infected and uninfected male mosquitoes as a function of the female mosquitoes, and we reduce the 4-ODE model to a 2-ODE model (subsection 3.3). The resulting 2-ODE system captures the key features of the original full system of nonlinear equations in the physically relevant parameter space.

At each model reduction step, we define the parameters for the reduced models in terms of the ones in the more accurate model, and we specify all the assumptions we make throughout the approximation steps. This systematic approach allows for all the parameters in the reduced model to be defined in terms of the epidemiologically relevant parameters for the 9-ODE model. It also creates an explicit relationship between the model parameters and solutions and allows us to reconstruct approximated solutions for all of the intermediate models as a function of the 2-ODE solutions.

We will evaluate the quality of the approximation by identifying the associated important dimensionless numbers (subsection 4.1) and analyzing the critical threshold condition (subsection 4.2) and phase plane dynamics (subsection 4.3). We also compare the numerical solutions (subsection 4.4) and the sensitivity indices (subsection 4.5) between the full model and the reduced models.

The analytic and numerical comparisons show that our reduced models

- preserve the key dimensionless numbers, including the basic reproductive number $\mathbb{R}_0$, the basic next generation numbers for the infected and uninfected populations,
- accurately capture the backward bifurcation and the critical threshold condition for having a stable *Wolbachia* epidemic in wild mosquitoes,
- exhibit similar transient behaviors using the phase plane analysis, and
- identify the same order of relative significance for the model parameters during the sensitivity analysis.

2. Review of the 9-ODE Transmission Model. The 9-ODE compartmental ODE model (Figure 2.1) divides the lifecycle of a mosquito into an aquatic state (combined eggs, larvae, and pupae stage), a single-adult state (for both males and females), and three possible pregnant states for females. The infection persists because a fraction, v_w, of the pregnant infected females transmit the bacteria maternally through a complex sexual cycle to their infected offspring in the aquatic state. Horizontal (mosquito-to-mosquito) transmission is rare and ignored in the model.

When an uninfected female mosquito becomes pregnant from an uninfected male mosquito, all of the offspring are uninfected. However, because of the cytoplasmic incompatibility, when an uninfected female mosquito becomes pregnant from an infected male mosquito, she becomes sterile and has no offspring. The nonsterile pregnant females (F_{pu} and F_{pw}) produce eggs at rates ϕ_u and ϕ_w, respectively, forming the aquatic-stage population and developing into adult mosquitoes at a rate ψ. The aquatic-stage population is regularized by a carrying capacity that accounts for the limited environmental resources. Qu, Xue, and M. Hyman [11] provide a detailed description of the model parameters (Table 2.1) and maternal transmission cycle for *A. aegypti* mosquitoes infected with wMel *Wolbachia*.

The 9-ODE model in Figure 2.1 is represented by the following system of ODEs:

$$\frac{dA_u}{dt} = \boldsymbol{\eta_u} F_{pu} + v_u \boldsymbol{\eta_w} F_{pw} - (\mu_a + \psi) A_u \,, \tag{2.1a}$$

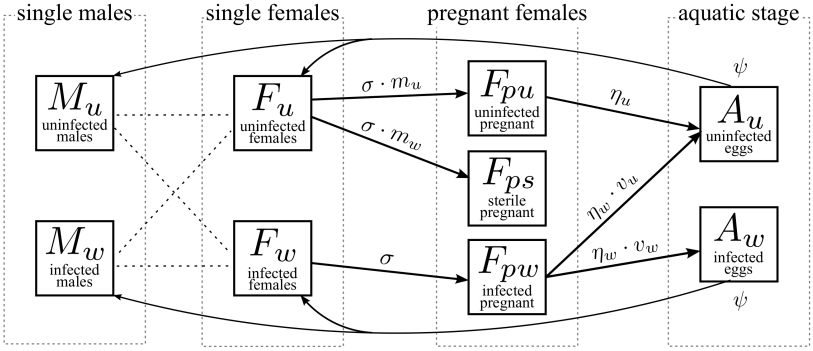

Fig. 2.1: Maternal transmission of *Wolbachia* in the mosquito population. Uninfected females, F_u, and *Wolbachia* infected females, F_w, are impregnated by either uninfected males, M_u or infected males, M_w, and enter the pregnant stage (with mating rate σ). Depending on the infection status of the partners, they can be uninfected pregnant F_{pu}, pregnant but sterile F_{ps} or infected pregnant F_{pw}. Pregnant females produce aquatic stage mosquitoes: uninfected pregnant females, F_{pu}, only produce uninfected individuals, A_u, (at rate $\boldsymbol{\eta_u}$); pregnant sterile females, F_{ps}, do not have any offspring; and infected pregnant females F_{pw} produce a fraction of v_w infected offspring A_w and a fraction of v_u uninfected offspring (at rate $\boldsymbol{\eta_w}$). The aquatic-stage mosquitoes hatch and emerge into adult forms (at rate ψ).

$$\frac{dA_w}{dt} = v_w\,\boldsymbol{\eta_w}\,F_{pw} - (\mu_a + \psi)A_w\,, \tag{2.1b}$$

$$\frac{dF_u}{dt} = b_f\psi A_u - (\sigma + \mu_{fu})F_u\,, \tag{2.1c}$$

$$\frac{dF_w}{dt} = b_f\psi A_w - (\sigma + \mu_{fw})F_w\,, \tag{2.1d}$$

$$\frac{dF_{pu}}{dt} = \sigma\,\boldsymbol{m_u}F_u - \mu_{fu}F_{pu}\,, \tag{2.1e}$$

$$\frac{dF_{ps}}{dt} = \sigma\,\boldsymbol{m_w}F_u - \mu_{fu}F_{ps}\,, \tag{2.1f}$$

$$\frac{dF_{pw}}{dt} = \sigma F_w - \mu_{fw}\,F_{pw}\,, \tag{2.1g}$$

$$\frac{dM_u}{dt} = b_m\psi A_u - \mu_{mu}M_u\,, \tag{2.1h}$$

$$\frac{dM_w}{dt} = b_m\psi A_w - \mu_{mw}M_w\,, \tag{2.1i}$$

where the hatching rates are defined as

$$\boldsymbol{\eta_u}(A_u, A_w) = \phi_u\Big(1 - \frac{A_u + A_w}{K_a}\Big)\,, \quad \boldsymbol{\eta_w}(A_u, A_w) = \phi_w\Big(1 - \frac{A_u + A_w}{K_a}\Big)\,,$$

and the fractions of uninfected and infected males are defined by

$$\boldsymbol{m_u} = M_u/(M_u + M_w)\,, \quad \boldsymbol{m_w} = 1 - \boldsymbol{m_u} = M_w/(M_u + M_w)\,.$$

To simplify the notation, we do not explicitly include the variable dependence in the bolded functions $\boldsymbol{\eta_u}(A_u, A_w)$, $\boldsymbol{\eta_w}(A_u, A_w)$, $\boldsymbol{m_u}(M_u, M_w)$, and $\boldsymbol{m_w}(M_u, M_w)$.

9-ODE model parameters		Baseline	Reference
b_f	Female birth probability	0.5	[14]
b_m	Male birth probability	0.5	[14]
σ	Per capita mating rate	1	[12]
ϕ_u	Per capita egg-laying rate for F_{pu}	13	[5, 8, 9]
ϕ_w	Per capita egg-laying rate for F_{pw}	11	[5, 17]
v_w	Maternal transmission rate	0.95	[17]
v_u	$= 1 - v_w$	0.05	[17]
ψ	Per capita development rate	1/8.75	[5, 17]
μ_a	Death rate for A_u or A_w	0.02	[5, 9, 17]
μ_{fu}	Death rate for F_u and F_{pu}	1/17.5	[8, 13]
μ_{fw}	Death rate for F_w and F_{pw}	1/15.8	[17]
μ_{mu}	Death rate for M_u	1/10.5	[8, 13]
μ_{mw}	Death rate for M_w	1/10.5	[8, 13]
K_a	Carrying capacity of aquatic stage	2×10^5	Estimated
$\boldsymbol{m_u} = M_u/(M_u + M_w)$		Fraction of uninfected males	
$\boldsymbol{\eta_u} = \phi_u(1 - (A_u + A_w)/K_a)$		Per capita reproduction rate for F_{pu}	
$\boldsymbol{\eta_w} = \phi_w(1 - (A_u + A_w)/K_a)$		Per capita reproduction rate for F_{pw}	

7-ODE model parameters	Definition
$\mu'_{fu} = \frac{\psi}{\psi+\mu_{fu}}\mu_{fu}$	Death rate for F_u and F_{pu}
$\mu'_{fw} = \frac{\psi}{\psi+\mu_{fw}}\mu_{fw}$	Death rate for F_w and F_{pw}
$\mu'_{mu} = \frac{\psi}{\psi+\mu_{mu}}\mu_{mu}$	Death rate for M_u
$\mu'_{mw} = \frac{\psi}{\psi+\mu_{mw}}\mu_{mw}$	Death rate for M_w
$\phi'_u = \frac{\psi}{\psi+\mu_a}\frac{\sigma+\mu'_{fu}}{\sigma+\mu_{fu}}\frac{\mu'_{fu}}{\mu_{fu}}\phi_u$	Per capita egg-laying rate for F_{pu}
$\phi'_w = \frac{\psi}{\psi+\mu_a}\frac{\sigma+\mu'_{fw}}{\sigma+\mu_{fw}}\frac{\mu'_{fw}}{\mu_{fw}}\phi_w$	Per capita egg-laying rate for F_{pw}
$K_p = b_f\frac{\psi}{\sigma+\mu'_{fu}}K_a$	Carrying capacity for single females
$\boldsymbol{\eta'_u} = \phi'_u(1 - (F_u + F_w)/K_p)$	Per capita reproduction rate for F_{pu}
$\boldsymbol{\eta'_w} = \phi'_w(1 - (F_u + F_w)/K_p)$	Per capita reproduction rate for F_{pw}

4-ODE model parameters	Definition
$\phi''_u = \frac{\sigma}{\sigma+\mu'_{fu}}\phi'_u$	Per capita egg-laying rate for F^u
$\phi''_w = \frac{\sigma}{\sigma+\mu'_{fw}}\phi'_w$	Per capita reproduction rate for F^w
$K_f = b_f\frac{\psi}{\mu'_{fu}}K_a$	Carrying capacity for females
$\boldsymbol{\eta''_u} = \phi''_u\,\boldsymbol{m_u}(1 - (F^u + F^w)/K_f)$	Per capita reproduction rate for F^u
$\boldsymbol{\eta''_w} = \phi''_w(1 - (F^u + F^w)/K_f)$	Per capita reproduction rate for F^w

2-ODE model parameters	Definition
$\boldsymbol{m'_u} = F^u/(F^u + \frac{\mu'_{fw}}{\mu'_{fu}}F^w)$	Approximated fraction of uninfected males
$\boldsymbol{\eta'''_u} = \phi''_u\,\boldsymbol{m'_u}(1 - (F^u + F^w)/K_f)$	Per capita reproduction rate for F^u

Table 2.1: All the parameters in the reduced models are defined in terms of the parameters for the full 9-ODE model. The rates have dimensions $days^{-1}$.

All of the progression rates are constant and have dimensions $days^{-1}$. This implies an exponential distribution for the time that the population takes to progress to the next stage and that the average time spent in a stage is the inverse of this rate. For example, the mean death rate for uninfected males is $\tau_{mu} = 1/\mu_{mu}$.

The system (2.1) is mathematically well-posed in the epidemiologically valid domain [11]

$$\mathcal{D} = \left\{ \begin{pmatrix} A_u \\ A_w \\ F_u \\ F_w \\ F_{pu} \\ F_{pw} \\ F_{ps} \\ M_u \\ M_w \end{pmatrix} \in \mathcal{R}^9 \;\middle|\; \begin{array}{c} A_u \geq 0, \\ A_w \geq 0, \\ 0 \leq A_u + A_w \leq K_a, \\ F_u \geq 0, \\ F_w \geq 0, \\ 0 \leq F_u + F_w \leq b_f \psi \frac{1}{\sigma+\mu_{fu}} K_a, \\ F_{pu} \geq 0, \\ F_{pw} \geq 0, \\ F_{ps} \geq 0, \\ 0 \leq F_{pu} + F_{pw} + F_{ps} \leq \frac{\sigma}{\sigma+\mu_{fu}} \frac{b_f \psi K_a}{\mu_{fu}}, \\ M_u \geq 0, \\ M_w \geq 0, \\ 0 \leq M_u + M_w \leq \frac{b_m \psi K_a}{\mu_{mu}} \end{array} \right\}. \tag{2.2}$$

2.1. Disease-Free Dimensionless Numbers for the 9-ODE model. When a small *Wolbachia* infection is introduced into a fully susceptible population, the transmission dynamics can be characterized by three dimensionless numbers:

- the basic next generation number for the uninfected population, $\mathbb{G}_{0u}$, is the number of uninfected eggs produced by one uninfected egg through one life-cycle;
- the basic next generation number for the infected population, $\mathbb{G}_{0w}$, is the number of infected eggs produced by one infected egg through one lifecycle; and
- the basic reproductive number, $\mathbb{R}_0^{(9)} = \mathbb{G}_{0w}^{(9)}/\mathbb{G}_{0u}^{(9)}$, is the average number of secondary infections a single *Wolbachia*-infected mosquito will cause when introduced into a fully susceptible population.

These quantities are derived in [11] and denoted by

$$\mathbb{G}_{0u}^{(9)} = b_f \frac{\psi}{\mu_a + \psi} \frac{\sigma}{\sigma + \mu_{fu}} \frac{\phi_u}{\mu_{fu}}, \quad \mathbb{G}_{0w}^{(9)} = v_w b_f \frac{\psi}{\mu_a + \psi} \frac{\sigma}{\sigma + \mu_{fw}} \frac{\phi_w}{\mu_{fw}}, \tag{2.3}$$

and

$$\mathbb{R}_0^{(9)} = v_w \frac{\mu_{fu}\phi_w(\sigma + \mu_{fu})}{\mu_{fw}\phi_u(\sigma + \mu_{fw})} = \frac{\mathbb{G}_{0w}^{(9)}}{\mathbb{G}_{0u}^{(9)}}. \tag{2.4}$$

These dimensionless numbers can be understood in terms of the products of the physically relevant factors described in [11]. The basic reproductive number $\mathbb{R}_0^{(9)}$ can be expressed as the ratio of growth of infected $\mathbb{G}_{0w}^{(9)}$ to uninfected eggs $\mathbb{G}_{0u}^{(9)}$.

2.2. Equilibrium States of the 9-ODE Model. There are three types of equilibria in system (2.1):

- a disease-free equilibrium (DFE), $EE^0 = (A_u^0, 0, F_u^0, 0, F_{pu}^0, 0, M_u^0, 0)$,

$$A_u^0 = K_a \left(1 - \frac{1}{\mathbb{G}_{0u}^{(9)}}\right), \qquad F_u^0 = b_f \frac{\psi}{\mu_{fu} + \sigma} A_u^0,$$

$$F^0_{pu} = b_f \frac{\psi\sigma}{(\mu_{fu}+\sigma)\mu_{fu}} A^0_u, \qquad M^0_u = b_m \frac{\psi}{\mu_{mu}} A^0_u\,,$$

- a complete-infection equilibrium (CIE), $EE^c = (0, A^c_w, 0, F^c_w, 0, F^c_{pw}, 0, M^c_w)$,

$$A^c_w = K_a\left(1 - \frac{1}{\mathbb{G}^{(9)}_{0w}}\right), \qquad F^c_w = b_f \frac{\psi}{\mu_{fw}+\sigma} A^c_w,$$
$$F^c_{pw} = b_f \frac{\psi\sigma}{(\mu_{fw}+\sigma)\mu_{fw}} A^c_w, \qquad M^c_w = b_m \frac{\psi}{\mu_{mw}} A^c_w\,,$$

- and endemic equilibrium (EE), $EE^* = (A^*_u, A^*_w, F^*_u, F^*_w, F^*_{pu}, F^*_{pw}, M^*_u, M^*_w)$,

$$A^*_u = \frac{K_a}{1+r_{wu}}\left(1 - \frac{1}{\mathbb{G}^{(9)}_{0w}}\right), \qquad A^*_w = r_{wu}\, A^*_u,$$
$$F^*_u = b_f \frac{\psi}{\sigma+\mu_{fu}} A^*_u, \qquad F^*_w = r_{wu}\, b_f \frac{\psi}{\sigma+\mu_{fw}} A^*_u,$$
$$F^*_{pu} = \frac{1}{1+r_{wu}}\, b_f \frac{\psi\sigma}{(\sigma+\mu_{fu})\mu_{fu}} A^*_u, \qquad F^*_{pw} = r_{wu}\, b_f \frac{\psi\sigma}{(\sigma+\mu_{fw})\mu_{fw}} A^*_u,$$
$$M^*_u = b_m \frac{\psi}{\mu_{mu}} A^*_u, \qquad M^*_w = r_{wu}\, b_m \frac{\psi}{\mu_{mw}} A^*_u\,,$$

and

$$F^*_{ps} = \frac{r_{wu}}{1+r_{wu}} b_f \frac{\psi\sigma}{(\sigma+\mu_{fu})\mu_{fu}} A^*_u\,.$$

The dimensionless ratio $r_{wu} > 0$ is a root of the following quadratic equation:

$$\frac{v_u}{v_w} r^2_{wu} + \left(\frac{v_u}{v_w} - 1\right) r_{wu} + \frac{1 - \mathbb{R}^{(9)}_0}{\mathbb{R}^{(9)}_0} = 0. \tag{2.5}$$

The CIE, EE^c, only exists when we have perfect maternal transmission rate ($v_w = 1$), and in this case, the equation (2.5) degenerates to a linear equation and has only one root that corresponds to one EE^* . If the maternal transmission is imperfect ($v_w < 1$), there are two roots for (2.5), which result in two EEs: one high-infection EE (denoted by EE^+) and one low-infection EE (denoted by EE^-).

2.3. Backward bifurcation and threshold condition. The stability analysis of the multiple equilibria is used to characterize the backward bifurcation in Figure 2.2, where the vertical axis is the fraction of infection in females. When having perfect maternal transmission ($v_w = 1$, left plot), there is a stable CIE, a stable DFE, and an unstable intermediate EE^*, which serves as a threshold condition for establishing endemic *Wolbachia*. Below the threshold state, the infected mosquitoes that have been introduced to the environment are wiped out by the wild population, and the system goes back to DFE; above the threshold state, the infection is able to gradually invade the wild environment, and at some point, the stable CIE is achieved.

When the maternal transmission is not perfect ($v_w < 1$, Figure 2.2, right plot), then the CIE becomes a stable high-infection EE^+, where both the uninfected and infected mosquitoes co-exist in the environment, and unstable low-infection state EE^- serves as the threshold condition.

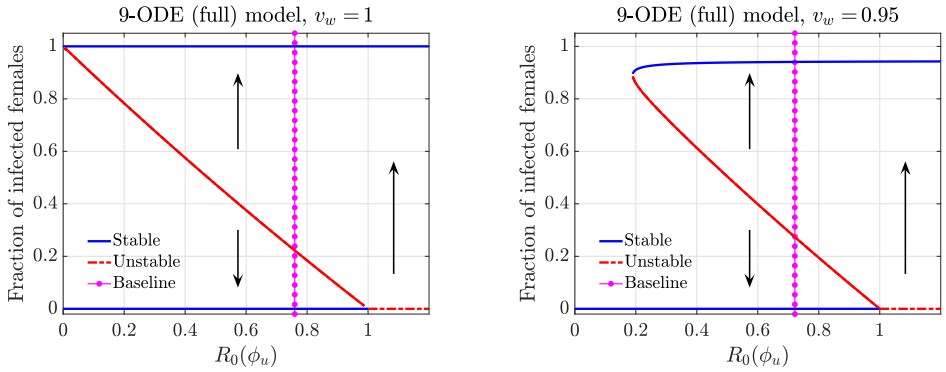

Fig. 2.2: For the full 9-ODE model, the threshold conditions for having a stable endemic state are characterized by these bifurcation diagrams for perfect (left) and imperfect (right) maternal transmission. We traced out these curves by varying the parameter ϕ_u and keeping other parameters (except the maternal transmission rate v_w) at the baseline values. The blue solid curves correspond to the stable EE^+, and the red dashed curves represent the unstable low-infection EE^-, which creates a threshold condition for establishing endemic *Wolbachia*. Below the threshold, the infection could not sustain and die out; Above the threshold, the infection develops and eventually achieve the high-infection stable EE^+. We note that although, the state EE^+ is insensitive to varying $\mathbb{R}_0$ as a function of ϕ_u, it is sensitive to $\mathbb{R}_0$ when varied as a function of other parameters, such as v_w.

In our analysis, we consider the sterile pregnant female mosquitoes, F_{ps}, as uninfected mosquitoes since they do not contribute to the maternal transmission cycle. That is, we define the fraction of "infected females" as the ratio

$$\mathcal{F}_f = \frac{F_w + F_{pw}}{F_u + F_{pu} + F_{ps} + F_w + F_{pw}} .$$

Note that this key dimensionless quantity differs slightly from the analysis in [11], where the F_{ps} group mosquitoes were treated as infected mosquitoes. This new definition simplifies the derivation of the reduced models.

3. Model Reductions. The 9-ODE model (2.1) offers important insights into using *Wolbachia* as a potential mitigation strategy. However, it is difficult to analyze a system of nine differential equations, especially when adding additional effects such as spatial heterogeneity. This has motivated us to create a hierarchy of reduced models based on assumptions that hold for a range of parameters and initial conditions appropriate for real-world applications. When deriving the reduced equations, we will strive to preserve as many key dimensionless quantities as possible and faithfully capture the backward bifurcation and threshold conditions. Also, the reduced model parameters and initial conditions will all be defined in terms of physically relevant 9-ODE model parameters.

The reduced models cannot capture all of the possible dynamics of the 9-ODE model over all possible parameter ranges and initial conditions. In our analysis, we will concentrate on preserving the key properties near the baseline values with the caveat that the reduced model may not be valid for parameter values far from these baseline

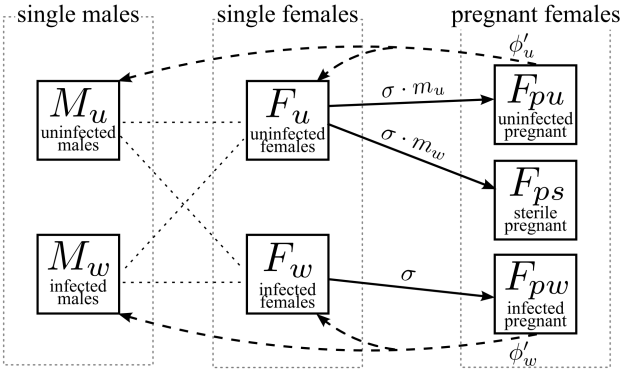

Fig. 3.1: Reduced 7-ODE model: Starting from the full baseline model in Figure 2.1, we remove the aquatic stages A_u and A_w, and let the pregnant females reproduce offspring that are directly enter the adult stages at a newly defined egg-laying rates ϕ'_u and ϕ'_w for uninfected and infected group, respectively. We also incorporate the delay in aquatic stages of the full model by adjusting the death rates of the adult stages in the reduced model, so that we have consistent timescales of one generation between the full model and this reduced model.

values. The key quantities we will approximately conserve in the reduced models include the basic next generation numbers $\mathbb{G}_{0u}$ and $\mathbb{G}_{0w}$ in (2.3), basic reproduction number $\mathbb{R}_0$ in (2.4), and the threshold condition for establishing stable *Wolbachia* epidemic, which is realized as the bifurcation diagram in Figure 2.2.

After describing the step-by-step reduction process, we will compare the reduced models to the full baseline model and show that the reduced models still capture the important properties of the original system in the next section (section 4).

3.1. The 7-ODE model: removing the aquatic stage. The aquatic-state populations do not directly contribute to the transmission dynamics and are a logical place to consider when reducing the number of variables. Thus, we simplify the 9-ODE model (2.1) by first removing the aquatic stages A_u and A_w. That is, we assume that the surviving eggs hatch instantaneously (with large egg development rate ψ) and progress directly into the adult mosquitoes, see Figure 3.1. However, the aquatic stage does contribute to the time duration for one generation of mosquitoes, and the number of new offspring reproduced in one generation. These are quantities we need to preserve in our reduced models.

When removing the aquatic stages, to keep the same timescale for one generation, we account for the significant amount of time the mosquitoes spend in the aquatic stage by modifying the death rates for the adult mosquitoes. Since the egg hatching rate, ψ, is constant, the distribution of time that it takes the eggs to hatch is exponentially distributed. The mean time for the eggs to hatch is, therefore, $\tau_\psi = 1/\psi$. In the full model, the entire lifespan of an uninfected female mosquito includes the delay spent in the aquatic stage, τ_ψ, and the time spent in the adult stage, $\tau_{fu} = 1/\mu_{fu}$. Thus, for the reduced 7-ODE model, to preserve this average mosquito lifetime we define $\tau'_{fu} = 1/\mu'_{fu} := \tau_\psi + \tau_{fu}$. Solving this equation for the death rate for the

modified uninfected females in the 7-ODE model, μ'_{fu}, we have

$$\mu'_{fu} = \frac{\psi}{\mu_{fu} + \psi}\mu_{fu}\,.$$

The modified death rates for the infected females, μ'_{fw}, uninfected males, μ'_{mu}, and infected males, μ'_{mw}, are all defined by the same approach (Table 2.1).

The basic next generation numbers for the 7-ODE model (Figure 3.1) describe the number of new uninfected and infected offspring reproduced by one uninfected and infected female around the zero-infection steady state:

$$\mathbb{G}^{(7)}_{0u} = b_f \frac{\sigma}{\sigma + \mu'_{fu}} \frac{\phi'_u}{\mu'_{fu}} \quad \text{and} \quad \mathbb{G}^{(7)}_{0w} = v_w b_f \frac{\sigma}{\sigma + \mu'_{fw}} \frac{\phi'_w}{\mu'_{fw}}\,, \tag{3.1}$$

where ϕ'_u and ϕ'_w are the new egg-laying rates for the uninfected and infected pregnant females in the 7-ODE model. The fractions $\sigma/(\sigma + \mu'_{fu})$ and $\sigma/(\sigma + \mu'_{fw})$ are the fractions of uninfected or infected single females that successfully mate and enter one of the pregnant stages before they die. The ratios ϕ'_u/μ'_{fu} and ϕ'_w/μ'_{fw} are the numbers of new offspring that an uninfected or infected pregnant female can reproduce throughout life. From there, all the offspring reproduced by the uninfected pregnant females are uninfected, b_f of which are females. For the infected population, a fraction of v_w offspring reproduced by infected pregnant females are infected through maternal transmission, b_f of which become females.

Because the basic next generation number $\mathbb{G}^{(7)}_{0u}$ is defined around the zero-infection state, $\boldsymbol{m_u} = 1$ and female mosquitos, F_u, can only mate with an uninfected male M_u. These mosquitoes become uninfected pregnant females, F_{pu}, and not sterile pregnant females, F_{ps}. Therefore, the fraction $\boldsymbol{m_u}$ does not show up in the fraction $\sigma/(\sigma+\mu'_{fu})$ for $\mathbb{G}^{(7)}_{0u}$.

We require the basic next generation number of the 7-ODE (3.1) to be the same as the 9-ODE model (2.3). This can be achieved by defining the 7-ODE egg-laying rates as

$$\phi'_u = \frac{\psi}{\psi + \mu_a} \frac{\sigma + \mu'_{fu}}{\sigma + \mu_{fu}} \frac{\mu'_{fu}}{\mu_{fu}} \phi_u \quad \text{and} \quad \phi'_w = \frac{\psi}{\psi + \mu_a} \frac{\sigma + \mu'_{fw}}{\sigma + \mu_{fw}} \frac{\mu'_{fw}}{\mu_{fw}} \phi_w\,.$$

This definition accounts for the fraction of deaths that happen during the aquatic stage $\psi/(\psi + \mu_a)$ and adjusts for the different death rates between the models using the ratios between death rates in the full model and reduced 7-ODE model.

We move the carrying capacity from the aquatic equations to the single female equations, so that the regularization is based on the total single female population $F_u + F_w$. This can be interpreted as limiting the availability of breeding sites for the single females. This results in the modified birth rates,

$$\boldsymbol{\eta'_u}(F_u\,, F_w) = \phi'_u\Big(1 - \frac{F_u + F_w}{K_p}\Big) \text{ and} \tag{3.2}$$

$$\boldsymbol{\eta'_w}(F_u\,, F_w) = \phi'_w\Big(1 - \frac{F_u + F_w}{K_p}\Big)\,, \tag{3.3}$$

where K_p is the carrying capacity for single females,

$$K_p = b_f \frac{\psi}{\sigma + \mu'_{fu}} K_a\,. \tag{3.4}$$

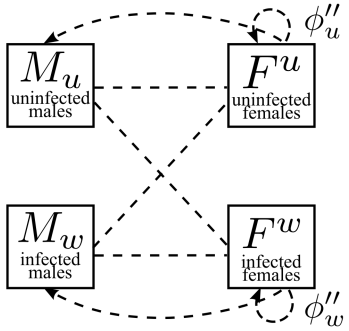

Fig. 3.2: Reduced 4-ODE model: From the 7-ODE model Figure 3.1, we reduce the scale of the model further by combining the infection groups of uninfected and infected females and defining uninfected females $F^u = F_u + F_{pu} + F_{ps}$ and infected females $F^w = F_w + F_{pw}$. We modify the reproduction rates for the uninfected and infected females, ϕ''_u and ϕ''_w, respectively.

The reduced 7-ODE model is

$$\frac{dF_u}{dt} = b_f \boldsymbol{\eta'_u} F_{pu} + v_u b_f \boldsymbol{\eta'_w} F_{pw} - (\sigma + \mu'_{fu}) F_u \,, \tag{3.5a}$$

$$\frac{dF_w}{dt} = v_w b_f \boldsymbol{\eta'_w} F_{pw} - (\sigma + \mu'_{fw}) F_w \,, \tag{3.5b}$$

$$\frac{dF_{pu}}{dt} = \sigma \boldsymbol{m_u} F_u - \mu'_{fu} F_{pu} \,, \tag{3.5c}$$

$$\frac{dF_{ps}}{dt} = \sigma \boldsymbol{m_w} F_u - \mu'_{fu} F_{ps} \,. \tag{3.5d}$$

$$\frac{dF_{pw}}{dt} = \sigma F_w - \mu'_{fw} F_{pw} \,, \tag{3.5e}$$

$$\frac{dM_u}{dt} = b_m \boldsymbol{\eta'_u} F_{pu} + v_u b_m \boldsymbol{\eta'_w} F_{pw} - \mu'_{mu} M_u \,, \tag{3.5f}$$

$$\frac{dM_w}{dt} = v_w b_m \boldsymbol{\eta'_w} F_{pw} - \mu'_{mw} M_w \,. \tag{3.5g}$$

Note that all the parameters for the 7-ODE model are defined in terms of the 9-ODE model parameters, as summarized in Table 2.1. The well-posed domain for the 7-ODE model is similar to the 9-ODE model (2.2) using the 7-ODE parameters.

3.2. The 4-ODE model: combining the infection groups. Single female mosquitoes become pregnant soon after emerging from their aquatic stage. Also, during this short time of being nonpregnant, they do not affect *Wolbachia* transmission. Therefore, to further reduce the model, we combine the pregnant and nonpregnant female groups and define the 4-ODE uninfected females, $F^u := F_u + F_{pu} + F_{ps}$, and infected females, $F^w := F_w + F_{pw}$ (Figure 3.2).

The new egg-laying rates, ϕ''_u and ϕ''_w, for the uninfected and infected groups are defined by matching the basic next generation numbers of the 7-ODE (3.1) and 4-ODE models,

$$\mathbb{G}^{(4)}_{0u} := b_f \frac{\phi''_u}{\mu'_{fu}} \,, \quad \text{and} \quad \mathbb{G}^{(4)}_{0w} := v_w b_f \frac{\phi''_w}{\mu'_{fw}} \,, \tag{3.6}$$

which gives

$$\phi_u'' = \frac{\sigma}{\sigma + \mu_{fu}'}\phi_u' , \quad \text{and} \quad \phi_w'' = \frac{\sigma}{\sigma + \mu_{fw}'}\phi_w' .$$

The basic next generation number, $\mathbb{G}_{0u}$, is defined at the disease-free equilibrium ($\boldsymbol{m_u} = 1$) and is only valid when there are a few infected mosquitoes. As the *Wolbachia* epidemic progresses ($\boldsymbol{m_u} < 1$), new uninfected offspring are only born when a single uninfected female mates with an uninfected male, which happens with probability $\boldsymbol{m_u} < 1$. To analyze this situation after an epidemic is in progress, we generalize the basic next generation number to estimate the number of new uninfected offspring reproduced through one generation at any time of the epidemic, $\mathbb{G}_u$. For the 7-ODE and 4-ODE models, the next generation number is

$$\mathbb{G}_u^{(7)} := b_f \frac{\sigma\, \boldsymbol{m_u}}{\sigma + \mu_{fu}'} \frac{\phi_u'}{\mu_{fu}'} = b_f \frac{\phi_u^*}{\mu_{fu}'} =: \mathbb{G}_u^{(4)} , \tag{3.7}$$

and ϕ_u^* is the adjusted birth rate for uninfected pregnant females to account for when they could become sterile after sex with a *Wolbachia* infected male. In (3.7), the fraction $\sigma\, \boldsymbol{m_u}/(\sigma + \mu_{fu}')$ represents the probability for a single uninfected female to successfully mate with an uninfected male and then become an uninfected pregnant female F_{pu}. At the disease-free equilibrium ($\boldsymbol{m_u} = 1$), $\mathbb{G}_u^{(7)}|_{t=0} = \mathbb{G}_{0u}^{(7)}$, which is the basic next generation number defined in (3.1).

Solving (3.7) for the adjusted birth rate for the uninfected population, ϕ_u^*, we have

$$\phi_u^* = \frac{\sigma\, \boldsymbol{m_u}}{\sigma + \mu_{fu}'}\phi_u' = \phi_u''\, \boldsymbol{m_u} . \tag{3.8}$$

Next, we approximate the carrying capacity for the entire female population based on the sum of the upper bounds of pregnant females and single females in invariant domain (2.2). We define the carrying capacity for the female mosquitoes as

$$K_f = b_f \frac{\psi}{\mu_{fu}'} K_a$$

and the resulting birth rates as

$$\boldsymbol{\eta_u''}(F^u, F^w) = \phi_u''\, \boldsymbol{m_u}\Big(1 - \frac{F^u + F^w}{K_f}\Big) \text{ and } \quad \boldsymbol{\eta_w''}(F^u, F^w) = \phi_w''\Big(1 - \frac{F^u + F^w}{K_f}\Big) . \tag{3.9}$$

The reduced 4-ODE model is

$$\frac{dF^u}{dt} = b_f \boldsymbol{\eta_u''} F^u + v_u b_f \boldsymbol{\eta_w''} F^w - \mu_{fu}' F^u , \tag{3.10a}$$

$$\frac{dF^w}{dt} = v_w b_f \boldsymbol{\eta_w''} F^w - \mu_{fw}' F^w , \tag{3.10b}$$

$$\frac{dM_u}{dt} = b_m \boldsymbol{\eta_u''} F^u + v_u b_m \boldsymbol{\eta_w''} F^w - \mu_{mu}' M_u , \tag{3.10c}$$

$$\frac{dM_w}{dt} = v_w b_m \boldsymbol{\eta_w''} F^w - \mu_{mw}' M_w , \tag{3.10d}$$

and the parameters are summarized in Table 2.1.

3.3. The 2-ODE model: removing the males. We analyzed the solutions of the 4-ODE model to identify combinations of the variables that are slowly varying and could be used as a constraint to reduce the number of independent variables. Moreover, the mosquito-borne diseases are transmitted by female mosquitoes through blood-meal bites. This leads us to consider approximating the fraction of uninfected males, $\boldsymbol{m_u}$, as a function of the uninfected and infected females and identify a 2-ODE system for just the female mosquitoes. We made the simplifying realistic assumptions that an equal number of infected male and female mosquitoes are born, and the ratio between the male and female infected mosquitoes only changes because of the differences in the death rates. This biological intuition motivates the following approximation:

$$\boldsymbol{m'_u} := \frac{F^u}{F^u + \frac{\mu'_{fw}}{\mu'_{fu}} F^w} \approx \frac{M_u}{M_u + M_w} = \boldsymbol{m_u}\,. \tag{3.11}$$

The ratio of female death rates μ'_{fw}/μ'_{fu} has been chosen to match the threshold conditions for the 2-ODE model to the 4-ODE model (which will be verified in section 4), and no male death rates show up due to the assumption of equal death rates for uninfected and infected male, $\mu_{mu} = \mu_{mw}$. Note that this approach could be modified for situations where the birth rates for males and females are not equal, and if the death rates for uninfected and infected males were different.

Moreover, numerical simulations (Figure 3.3) show that the approximation (3.11) is reasonably good given appropriate initial conditions: for both simulations, we have picked the initial conditions that satisfy (3.11) exactly at $t = 0$, that is, $(F^w/M_w)|_{t=0} = \frac{\mu'_{fu}}{\mu'_{fw}} F^0_u/M^0_u$, where (F^0_u, M^0_u) are the DFE steady states for uninfected females and males in the 4-ODE model. (See (4.1) derived in the next section.)

We then use the approximation (3.11) to modify the birth rates $\boldsymbol{\eta''_u}$ in (3.9) as

$$\boldsymbol{\eta'''_u}(F^u, F^w) = \phi''_u \boldsymbol{m'_u}\Big(1 - \frac{F^u + F^w}{K_f}\Big)\,,$$

and the reduced 2-ODE model for *Wolbachia* transmission in female mosquitoes is written as

$$\frac{dF^u}{dt} = b_f \boldsymbol{\eta'''_u} F^u + v_u b_f \boldsymbol{\eta''_w} F^w - \mu'_{fu} F^u\,, \tag{3.12a}$$

$$\frac{dF^w}{dt} = v_w b_f \boldsymbol{\eta''_w} F^w - \mu'_{fw} F^w\,. \tag{3.12b}$$

Using the definitions for the coefficients, these equations can be expressed in terms of the original 9-ODE parameters as

$$\frac{dF^u}{dt} = c_{u1} \frac{F^u}{F^u + c_{wu} F^w}\Big(1 - \frac{F^u + F^w}{K_f}\Big) F^u + c_{u2}\Big(1 - \frac{F^u + F^w}{K_f}\Big) F^w - c_{u3} F^u\,,$$

$$\frac{dF^w}{dt} = c_{w1} \frac{F^u}{F^u + c_{wu} F^w}\Big(1 - \frac{F^u + F^w}{K_f}\Big) F^w - c_{w2} F^w\,,$$

where

$$c_{u1} = b_f \frac{\psi}{\psi + \mu_a} \frac{\psi}{\psi + \mu_{fu}} \frac{\sigma}{\sigma + \mu_{fu}} \phi_u, \qquad c_{u2} = v_u b_f \frac{\psi}{\psi + \mu_a} \frac{\psi}{\psi + \mu_{fw}} \frac{\sigma}{\sigma + \mu_{fw}} \phi_w,$$

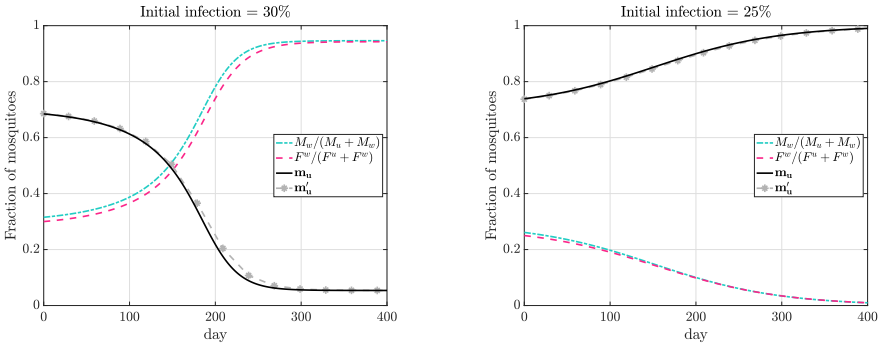

Fig. 3.3: Numerical simulations for the 4-ODE system with two balanced initial conditions. The black solid curves are the fraction of uninfected males $\boldsymbol{m_u}$, and the grey dashed curves with asterisks are the approximated ratio, $\boldsymbol{m'_u}$, that use the female population. For both initial conditions, the approximation $\boldsymbol{m'_u}$ is close to $\boldsymbol{m_u}$, which justifies our assumption in (3.11).

$$c_{w1} = v_w b_f \frac{\psi}{\psi+\mu_a}\frac{\psi}{\psi+\mu_{fw}}\frac{\sigma}{\sigma+\mu_{fw}}\phi_w, \qquad c_{wu} = \frac{\mu_{fw}}{\mu_{fu}}\frac{\psi+\mu_{fu}}{\psi+\mu_{fw}},$$

$$c_{u3} = \frac{\psi}{\psi+\mu_{fu}}\mu_{fu}, \quad c_{w2} = \frac{\psi}{\psi+\mu_{fw}}\mu_{fw}, \qquad K_f = b_f\Big(1+\frac{\psi}{\mu_{fu}}\Big)K_a\,.$$

We now have a hierarchy of reduced models approximating the original 9-ODE model at different scales. We derived the 2-ODE model for the female population with quadratic nonlinear terms as birth rates. The parameters for the reduced models are all defined as explicit combinations of the ones in the more accurate models (see Table 2.1).

We considered reducing the model further to a single ODE by assuming that the total population size is in equilibrium. We decided not to continue our model reduction since this equilibrium depends on the fraction of *Wolbachia* infection in the population, and the model would not be appropriate for prediction when releasing new infected mosquitoes, using insecticide to reduce the overall mosquito population, or for a time-dependent carrying capacity.

4. Model Comparisons. We will evaluate the quality of the approximation at each step by identifying the important dimensionless numbers and analyzing the critical threshold condition for each reduced model.

Note that in the following descriptions, for simplicity of presentation, we have used the same notation to represent the equilibrium points across different reduced models, and we will make it clear based on the context when referring to any of them.

4.1. Comparing dimensionless numbers. We derive the expressions of the dimensionless numbers and steady states for each reduced model, and we summarize the basic next generation numbers and the basic reproductive numbers for all the models in Table 4.1. Using the parameter definitions in Table 2.1, these dimensionless numbers all agree with the full 9-ODE model.

9-ODE	7-ODE	4-ODE	2-ODE
$\mathbb{G}_{0w} = v_w b_f \frac{\psi}{\mu_a+\psi}\frac{\sigma}{\sigma+\mu_{fw}}\frac{\phi_w}{\mu_{fw}}$	$= v_w b_f \frac{\sigma}{\sigma+\mu'_{fw}}\frac{\phi'_w}{\mu'_{fw}}$	$= v_w b_f \frac{\phi''_w}{\mu'_{fw}}$	$= v_w b_f \frac{\phi''_w}{\mu'_{fw}}$
$\mathbb{G}_{0u} = b_f \frac{\psi}{\mu_a+\psi}\frac{\sigma}{\sigma+\mu_{fu}}\frac{\phi_u}{\mu_{fu}}$	$= b_f \frac{\sigma}{\sigma+\mu'_{fu}}\frac{\phi'_u}{\mu'_{fu}}$	$= b_f \frac{\phi''_u}{\mu'_{fu}}$	$= b_f \frac{\phi''_u}{\mu'_{fu}}$
$\mathbb{R}_0 = v_w \frac{\mu_{fu}\,\phi_w\,(\sigma+\mu_{fu})}{\mu_{fw}\,\phi_u\,(\sigma+\mu_{fw})}$	$= v_w \frac{\mu'_{fu}\,\phi'_w\,(\sigma+\mu'_{fu})}{\mu'_{fw}\,\phi'_u\,(\sigma+\mu'_{fw})}$	$= v_w \frac{\mu'_{fu}\,\phi''_w}{\mu'_{fw}\,\phi''_u}$	$= v_w \frac{\mu'_{fu}\,\phi''_w}{\mu'_{fw}\,\phi''_u}$

Table 4.1: Dimensionless numbers $\mathbb{G}_{0w}$, $\mathbb{G}_{0u}$, and $\mathbb{R}_0$ are identical for all the models given the parameter definition in Table 2.1.

4.1.1. The 7-ODE Model. Following the same approach as in [11], the basic next generation numbers for the 7-ODE model are

$$\begin{aligned}
\mathbb{G}^{(7)}_{0u} &= \text{Prob}(F_u \to F_{pu}) \times (\#\ F_u \text{ generated by} F_{pu}) \\
&= \left(\frac{\sigma}{\sigma+\mu'_{fu}}\right)\left(b_f\frac{\phi'_u}{\mu'_{fu}}\right) = b_f\frac{\sigma}{\sigma+\mu'_{fu}}\frac{\phi'_u}{\mu'_{fu}}\,, \\
\mathbb{G}^{(7)}_{0w} &= \text{Prob}(F_w \to F_{pw}) \times (\#\ F_w \text{ generated by} F_{pw}) \\
&= \left(\frac{\sigma}{\sigma+\mu'_{fw}}\right)\left(v_w b_f\frac{\phi'_w}{\mu'_{fw}}\right) = v_w b_f\frac{\sigma}{\sigma+\mu'_{fw}}\frac{\phi'_w}{\mu'_{fw}}\,.
\end{aligned}$$

The DFE for the 7-ODE model is $EE^0 = (F^0_u, 0, F^0_{pu}, 0, M^0_u, 0)$, where

$$F^0_u = K_p\left(1-\frac{1}{\mathbb{G}^{(7)}_{0u}}\right), \qquad F^0_{pu} = \frac{\sigma}{\mu'_{fu}}F^0_u,$$
$$M^0_u = \frac{\sigma+\mu'_{fu}}{\mu'_{mu}}F^0_u.$$

The CIE for perfect maternal transmission, $v_w = 1$, is $EE^c = (0, F^c_w, 0, F^c_{pw}, 0, M^c_w)$, where

$$F^c_w = K_p\left(1-\frac{1}{\mathbb{G}^{(7)}_{0w}}\right), \qquad F^c_{pw} = \frac{\sigma}{\mu'_{fw}}F^0_w,$$
$$M^c_w = \frac{\sigma+\mu'_{fw}}{\mu'_{mw}}F^0_w.$$

The EE is $EE^* = (F^*_u, F^*_w, F^*_{pu}, F^*_{pw}, M^*_u, M^*_w)$, where

$$F^*_u = \frac{K_p}{1+r_{wu}\frac{\sigma+\mu'_{fu}}{\sigma+\mu'_{fw}}}\left(1-\frac{1}{\mathbb{G}^{(7)}_{0w}}\right),$$
$$F^*_w = r_{wu}\frac{\sigma+\mu'_{fu}}{\sigma+\mu'_{fw}}F^*_u\,, \qquad F^*_{pu} = \frac{1}{1+r_{wu}}\frac{\sigma}{\mu'_{fu}}F^*_u\,,$$

$$F^*_{pw} = r_{wu}\frac{\sigma(\sigma+\mu'_{fu})}{\mu'_{fw}(\sigma+\mu'_{fw})}F^*_u\,, \qquad F^*_{ps} = \frac{r_{wu}}{1+r_{wu}}\frac{\sigma}{\mu'_{fu}}F^*_u\,,$$

$$M^*_w = r_{wu}\frac{\sigma+\mu'_{fu}}{\mu'_{mw}}F^*_u\,, \qquad M^*_u = \frac{\sigma+\mu'_{fu}}{\mu'_{mu}}F^*_u\,.$$

The r_{wu} satisfies the same equation (2.5) as in the full model. Similar to the case for the 9-ODE model, when having imperfect transmission, there are two roots for r_{wu} solved from the quadratic equation (2.5), which are corresponding to two EEs; when having perfect transmission, there are one EE and one CIE instead.

Using the next generation matrix approach, we derive the basic reproductive number for the reduced 7-ODE system (3.5)

$$\mathbb{R}^{(7)}_0 = v_w\frac{\mu'_{fu}\,\phi'_w\,(\sigma+\mu'_{fu})}{\mu'_{fw}\,\phi'_u\,(\sigma+\mu'_{fw})} = \frac{\mathbb{G}^{(7)}_{0w}}{\mathbb{G}^{(7)}_{0u}}\,.$$

4.1.2. The 4-ODE model. The basic next generation numbers for the uninfected and infected population are

$$\mathbb{G}^{(4)}_{0u} = (\#\text{ of uninfected } F^u \text{ generated over the life span}) \times \text{Prob(female)} = b_f\frac{\phi''_u}{\mu'_{fu}}\,,$$

$$\mathbb{G}^{(4)}_{0w} = (\#\text{ of infected } F^w \text{ generated over the life span}) \times \text{Prob(female)} = v_w b_f\frac{\phi''_w}{\mu'_{fw}}\,.$$

The DFE for the 4-ODE system is $EE^0 = (F^0_u, 0, M^0_u, 0)$, where

$$F^0_u = \left(1-\frac{1}{\mathbb{G}^{(4)}_{0u}}\right)K_f,\ M^0_u = \frac{\mu'_{fu}}{\mu'_{mu}}\left(1-\frac{1}{\mathbb{G}^{(4)}_{0u}}\right)K_f. \tag{4.1}$$

The CIE ($v_w = 1$) is $EE^c = (0, F^c_w, 0, M^c_w)$, where

$$F^c_w = \left(1-\frac{1}{\mathbb{G}^{(4)}_{0w}}\right)K_f,\ M^c_w = \frac{\mu'_{fw}}{\mu'_{mw}}\left(1-\frac{1}{\mathbb{G}^{(4)}_{0w}}\right)K_f.$$

The EE is $EE^* = (F^*_u, F^*_w, M^*_u, M^*_w)$, where

$$F^*_u = \frac{K_f}{1+r_{wu}\frac{\mu'_{fu}}{\mu'_{fw}}}\left(1-\frac{1}{\mathbb{G}^{(4)}_{0w}}\right), \qquad F^*_w = r_{wu}\frac{\mu'_{fu}}{\mu'_{fw}}F^*_u,$$

$$M^*_u = \frac{\mu'_{fu}}{\mu'_{mu}}F^*_u, \qquad M^*_w = r_{wu}\frac{\mu'_{fu}}{\mu'_{mw}}F^*_u,$$

and r_{wu} is a solution of the quadratic equation (2.5) as in the 9-ODE model.

Using the next generation matrix approach, the basic reproductive number for the reduced system (3.10) is

$$\mathbb{R}^{(4)}_0 = v_w\frac{\mu'_{fu}\,\phi''_w}{\mu'_{fw}\,\phi''_u} = \frac{\mathbb{G}^{(4)}_{0w}}{\mathbb{G}^{(4)}_{0u}}\,.$$

4.1.3. The 2-ODE model. The basic next generation numbers $\mathbb{G}_{0u}^{(2)}$ and $\mathbb{G}_{0w}^{(2)}$ are the same for the 2-ODE and 4-ODE models. The DFE is $EE^0 = (F_u^0, 0)$,

$$F_u^0 = \left(1 - \frac{1}{\mathbb{G}_{0u}^{(2)}}\right) K_f \,,$$

and CIE is $EE^c = (0, F_w^0)$,

$$F_w^0 = \left(1 - \frac{1}{\mathbb{G}_{0w}^{(2)}}\right) K_f \,.$$

The EE is $EE^* = (F_u^*, F_w^*)$, where

$$F_u^* = \frac{K_f}{1 + r_{wu}\frac{\mu'_{fu}}{\mu'_{fw}}}\left(1 - \frac{1}{\mathbb{G}_{0w}^{(2)}}\right), \qquad F_w^* = r_{wu}\frac{\mu'_{fu}}{\mu'_{fw}}F_u^* \,,$$

where r_{wu} satisfies the same equation (2.5) as in the full model.

Using the next generation matrix approach, the basic reproductive number for the reduced system (3.12) is

$$\mathbb{R}_0^{(2)} = v_w \frac{\mu'_{fu}\,\phi''_w}{\mu'_{fw}\,\phi''_u} = \frac{\mathbb{G}_{0w}^{(2)}}{\mathbb{G}_{0u}^{(2)}} \,.$$

4.2. Comparing threshold conditions. The fraction of infection in females is $\mathcal{F}_f$ for the 9-ODE and 7-ODE model, and $\mathcal{F}'_f = F^w/(F^u + F^w)$ for the 4-ODE and 2-ODE models. The bifurcation diagrams for the fraction of infection in females as a function of the basic reproductive number $\mathbb{R}_0$ are plotted in Figure 4.1 for the perfect (top row) and imperfect (bottom row) maternal transmission cases.

The bifurcation curves for all the reduced models are almost indistinguishable. The zoom-in plot in the right column shows that there is an only small discrepancy between the full model and 7-ODE model near the baseline scenario, and all the reduced models (7-ODE, 4-ODE, and 2-ODE systems) have the same bifurcation curves.

The threshold ratio of infected females in the 9-ODE to sustain an epidemic,

$$\frac{F_w + F_{pw}}{F_u + F_{pu} + F_{ps}} = r_{wu}\frac{\mu_{fu}}{\mu_{fw}} \approx 0.38, \text{ threshold infection} \approx 27.35\% \,, \tag{4.2}$$

is almost identical to the threshold ratio for 7-ODE, 4-ODE, and 2-ODE models

$$\frac{F^w}{F^u} = r_{wu}\frac{\mu'_{fu}}{\mu'_{fw}} \approx 0.39, \text{ threshold infection} \approx 28.06\% \,. \tag{4.3}$$

These numerical values in (4.2) and (4.3) are the evaluations at the baseline case using values in Table 2.1.

4.3. Phase plane analysis. We now compare the transient behavior of the solutions for the models using a phase plane analysis for the dimensionless fractions of the population infected. The balanced initial conditions for the phase plane analysis are distributed among different groups in a way that is consistent with a natural

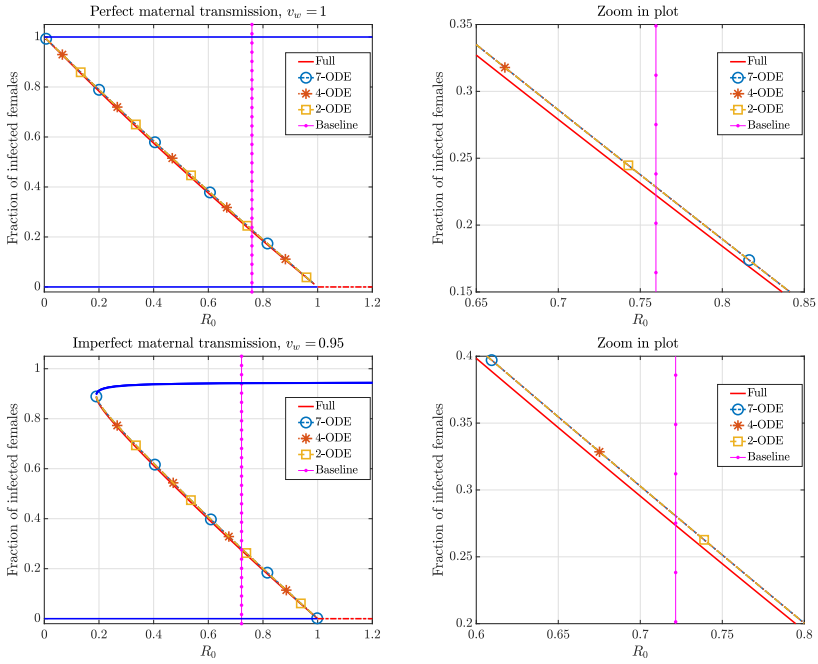

Fig. 4.1: Comparisons of bifurcation diagrams among the full and all the reduced models. Left column: backward bifurcation diagrams for all models; right column: zoom in plot around the baseline scenario. Top row: perfect maternal transmission case (we set $v_w = 1$ and keep the rest parameters at baseline values); bottom row: imperfect maternal transmission case (baseline case using parameters in Table 2.1). The bifurcation curves for different models are almost overlapping each over. From the zoom-in plot, we observe a tiny discrepancy in the unstable threshold levels between the full model and the reduced models. At the baseline setting, the threshold percentages to establish a stable EE infection in females are 27.35% for the full model and 28.06% for all the reduced models.

ongoing epidemic. We approximated these conditions by rescaling the balanced relationship among the different groups at the steady-state solutions. For example, in the 9-ODE model, given A_u and A_w, we derive the state variables for other compartments as follows:

$$
\begin{aligned}
F_u &= b_f \frac{\psi}{\mu_{fu}+\sigma} A_u, & F_w &= b_f \frac{\psi}{\mu_{fw}+\sigma} A_w,\\
M_u &= b_m \frac{\psi}{\mu_{mu}} A_u, & M_w &= b_m \frac{\psi}{\mu_{mw}} A_w,\\
F_{pu} &= b_f \frac{\psi\sigma}{(\sigma+\mu_{fu})\mu_{fu}} \frac{M_u}{M_u+M_w} A_u, & F_{pw} &= b_f \frac{\psi\sigma}{(\sigma+\mu_{fw})\mu_{fw}} A_w,\\
F_{ps} &= b_f \frac{\psi\sigma}{(\sigma+\mu_{fu})\mu_{fu}} \frac{M_w}{M_u+M_w} A_u.
\end{aligned}
\tag{4.4}
$$

To simplify scaling the phase-plane analysis to different populations sizes, we analyze the solution trajectories for two key dimensionless quantities: fraction of infection

in aquatic-stage mosquitoes and the total number of aquatic-stage mosquitoes relative to the carrying capacity. We prescribe different initial conditions on the phase plane that are above and below the carrying capacity and have various fractions of infection. The solution trajectories converge to the carrying capacity limit and then bifurcate and approach one of the two stable steady states: the DFE and or CIE.

Figures 4.2a and 4.2b show the phase plane dynamics for the 9-ODE model under perfect maternal transmission ($v_w = 1$). The y-axis is the fraction of carrying capacity for the aquatic stages. The x-axis is the fraction of females infected in Figure 4.2a and is the fraction of aquatic populations infected in Figure 4.2b. The bifurcation point (marked using a red star) is corresponding to the unstable EE. In Figure 4.2a, the fraction of infection in the females changes little as the population approaches the carrying capacity. The transient dynamics are more evident in the aquatic stages, as shown in Figure 4.2b. This may be due to the complicated lifecycle of mosquitoes, which serves as buffering layers that delay the response in the adult stages when there are changes happening in the aquatic stages.

The 2-ODE model (Figure 4.2c) phase plane (with fractions of females infected on the x-axis) is closer to Figure 4.2b because both of these plots compare the compartments that are directly regularized by the carrying capacity constraint.

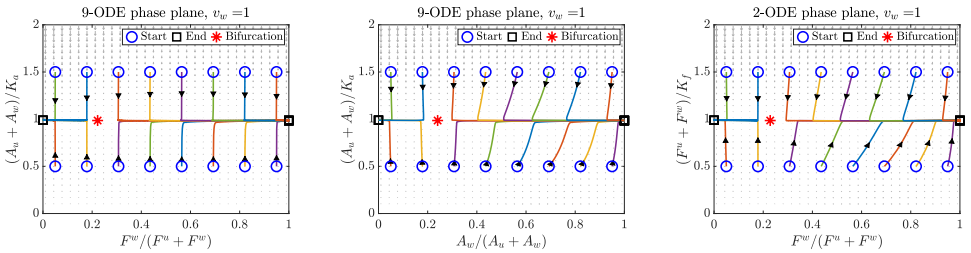

(a) (b) (c)

Fig. 4.2: Comparison of phase plane analysis between 9-ODE and 2-ODE models, given perfect maternal transmission ($v_w = 1$). The phase plane dynamics and solution trajectories are plotted using dimensionless quantities: the fraction of infection and total population size with respect to carrying capacity. The transient behaviors in the regularized groups are similar between 9-ODE (Figure 4.2b) and 2-ODE (Figure 4.2c). For the 9-ODE model, there is a delay in the development of infection in females when there are changes happening in the aquatic stages (Figure 4.2a).

4.4. Numerical Comparisons. We compare the numerical solutions of the reduced models through both a top-down, where we compare an aggregated solution of the 9-ODE model with the reduced model solutions, and bottom-up analysis, where we use the 2-ODE model solutions to approximate the 9-ODE solutions using the balanced relationships (4.4).

To minimize possible nonphysical initial rapid transients, we initialize the models with a balanced initial condition, as in subsection 4.3. However, since we don't have the total population size available, we use an alternative approach that is described in [6], where a very small number of infections are introduced to a system with $\mathbb{R}_0 > 1$ and the infection is allowed to grow to the desired initial infection level. Because $\mathbb{R}_0 < 1$ in our model, any small *Wolbachia* infection will die out. Therefore, we

introduce a small perturbation above the unstable low-infection EE and allow this infection to grow to the desired initial infection level.

If the simulation is for a field release of *Wolbachia* infected mosquitoes, where a large number of infected mosquitoes are released, then the initial conditions are not balanced. In this case, there will be a rapid transient process soon after the release. These transients might not be as accurately described using the reduced models as for the balanced initial conditions. Even so, after the initial transients, the solutions of different models converge.

4.4.1. Top-down comparison of the 9-ODE and reduced models. In the top-down approach, we aggregate the solutions of the 9-ODE model to compare them with the solutions of the reduced models. We create a balanced initial condition by perturbing the unstable low-infection EE by adding, or removing, one infected female mosquito and run the simulation until there is at least 1% of a change in the fraction of infection in females.

Figure 4.3a compares the solutions of the models for positive and negative perturbations about the EE. All the models show similar transient behavior between the initial conditions and the same high-infection endemic state or disease-free state. Moreover, there is some delay in the growing case for the 7-ODE model at the baseline setting. This delay is significantly reduced when doubling the parameter egg development rate ψ (Figure 4.3b). We further quantify this trend by evaluating the slopes of the curves (growth and clearance rates) for the 9-ODE and 2-ODE models and the time it takes for the infection to grow or decay (Table 4.2). The discrepancy is small enough for the 2-ODE model to give qualitatively similar behavior in situations where the dynamics are smooth.

We observed that the relative accuracy of reduced models depends on the specific simulation. Above the threshold condition in the 30% infection case, the differences between the reduced model and the 9-ODE model give the ranking 2-ODE>4-ODE>7-ODE. Below the threshold condition in the 25% infection case, the order is 7-ODE>4-ODE≈2-ODE.

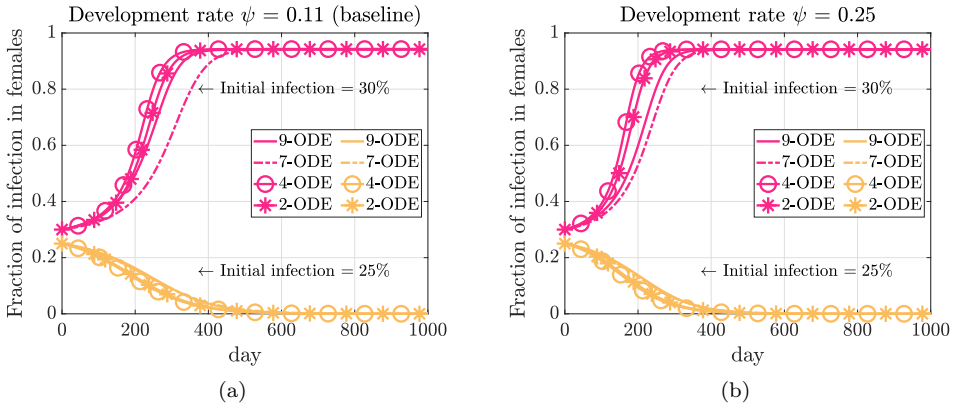

Fig. 4.3: Numerical simulations using the initial infections that are above and below the unstable EE threshold condition respectively. The fraction of infected females, ($\mathcal{F}_f$ or $\mathcal{F}'_f$), have the same initial growth rate and final steady states, but slightly different transient behavior.

	9-ODE	2-ODE
Growth rate at 35% (day^{-1})	0.081%	0.087%
Clearance rate at 25% (day^{-1})	-0.020%	-0.030%
Time from 40% to 80% infection (day)	138	118
Time from 25% to 10% infection (day)	286	242

Table 4.2: The 9-ODE and 2-ODE models have similar growth or clearance rates for initial conditions slightly above and below the threshold condition, respectively.

4.4.2. Bottom-up comparison of the 2-ODE and 9-ODE models. In the bottom-up approach, we use the analytic relationships that were used to define the reduced models to boost the reduced 2-ODE solutions and reconstruct approximated solutions for the more complex models. To reconstruct the solutions for all the compartments in the 9-ODE model from the reduced 2-ODE system (3.12), we use the balanced relationship described in (4.4) to define the 9-ODE model solutions in terms of the 2-ODE model ones. We then compare the reconstructed model with the full 9-ODE model in each group in Figure 4.4. The reconstructed model preserves the steady states in fractions and presents similar transition trends. Moreover, similar to the comparison in Figure 4.3, there is a delay in the 9-ODE model that could not be captured by the reconstructed model.

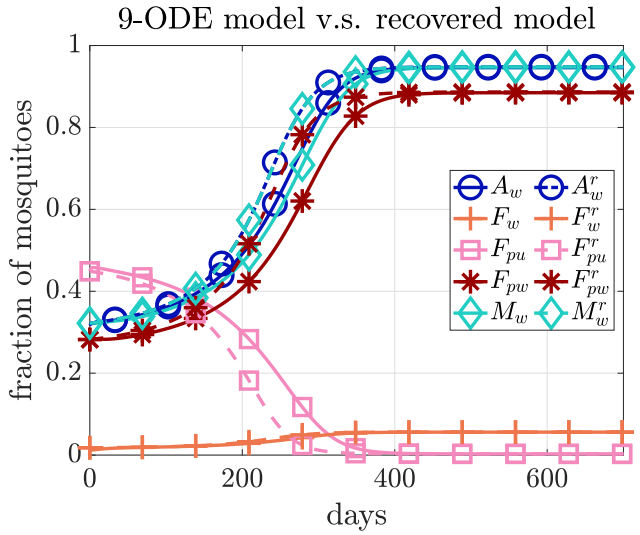

Fig. 4.4: Bottom-up comparison between the solutions of the full model and the reconstructed solution from the 2-ODE model using the balanced relationship between the groups. The reconstructed model preserves the steady states in fractions and presents similar transition trends.

4.5. Sensitivity Analysis. The model parameters in Table 2.1 represent our best-guess estimates for practical scenarios. However, it is difficult to obtain good estimates of the model parameters, and often the parameters would be more accurately

represented by a distribution of values, than a specific scalar. We use sensitivity analysis to quantify the relative significance of the model parameters by measuring the relative change in the output quantities of interests (QOIs) with respect to the perturbation on the input parameters of interests (POIs). We carry out the sensitivity analysis for each reduced model with respect to their relevant model parameters, and we compare how the reduced models are able to capture the relative significance in the parameters.

Following the framework in [2], we define the normalized relative sensitivity index of a QOI, $q(p)$, with respect to the POI, p, as

$$\mathcal{S}_p^q := \frac{p}{q} \times \frac{\partial q}{\partial p}\,.$$

The (relative) sensitivity index $\mathcal{S}_p^q$ measures the percentage change in the QOI given the percentage change in an input POI, that is, if parameter p changes by $x\%$, then quantity q changes by $\mathcal{S}_p^q \times x\%$. The sign of $\mathcal{S}_p^q$ determines if the response is increasing or decreasing. When evaluated at the baseline parameter values, $p = \hat{p}$ and $\hat{q} = q(\hat{p})$, the index,

$$\mathcal{S}_{\hat{p}}^q := \mathcal{S}_p^q\Big|_{p=\hat{p}} = \frac{\hat{p}}{\hat{q}} \times \frac{\partial q}{\partial p}\Big|_{p=\hat{p}},$$

is called the local (relative) sensitivity index of q at $\hat{p}$.

We calculate the local sensitivity indices for the following QOIs:

1. Basic reproductive number $\mathbb{R}_0$; the threshold conditions to establish a stable *Wolbachia* epidemic; and the endemic *Wolbachia* prevalence.
2. When the infection takes off, we consider the time from 40% to 80% infection in females and the growth rate at 35% infection.
3. When the infection dies out, we consider the time from 25% to 10% infection in females and the clearance rate at 25%.

For the QOIs in group 1, since we have explicit formulas (Table 4.1 for $\mathbb{R}_0$'s and the unstable low-infection EEs of the models), we derive the analytic expressions for the derivatives $\partial q/\partial p$ and sensitivity indices $\mathcal{S}_{\hat{p}}^q$ to each relevant parameter, which are then evaluated at the baseline values given in Table 2.1. For the QOIs in group 2 and 3, since the analytic derivatives for these quantities are not available, we numerically approximate the derivatives by using the finite difference method. (We have used center differences with 0.1% change in p around baseline values.)

We consider POIs to be all the parameters that are associated with female mosquitoes: maternal transmission rate (v_w), female death rates (μ_{fu} and μ_{fw} for the 9-ODE model and μ'_{fu} and μ'_{fw} for the 2-ODE model), egg-laying rates (ϕ_u and ϕ_w for the 9-ODE model ϕ''_u and ϕ''_w for the 2-ODE model), mating rate σ, hatching rate ψ, and death rates at aquatic stages μ_a. We list only the results for the 9-ODE model and the reduced 2-ODE model in Table 4.3. A complete comparison for all the reduced models is presented in Appendix A. We observe that the reduced 2-ODE model preserves the order of significance and closely approximates the index values for all the POIs: the maternal transmission rate v_w has the largest impact on all the QOIs except $\mathbb{R}_0$. Aside from v_w, the egg-laying rates (ϕ_*) have the most impact on the speed of establishment or clearance of *Wolbachia* epidemics (growth or clearance rate and time to achieve endemic or decay), and female death rates have the most impact on the final prevalence of *Wolbachia* infection.

Relative Sensitivity Indicies								
QOI / POI	Model	$\mathbb{R}_0$	Thresh cond.	Wolb. prev.	$T_{40\text{-}80\%}$ inf.	Growth at 35%	$T_{25\text{-}10\%}$ inf.	Clear. at 25%
μ_{fw}	9-ODE	-1.06	2.11	-0.06	1.52	-6.47	-10.87	25.65
μ'_{fw}	2-ODE	-1.00	1.93	-0.06	1.19	-6.27	-9.05	19.25
μ_{fu}	9-ODE	1.05	-2.09	0.06	-2.11	7.03	10.19	-24.87
μ'_{fu}	2-ODE	1.00	-1.93	0.06	-2.20	7.29	8.06	-18.26
v_w	9-ODE	1.00	-3.87	1.29	-7.62	15.59	16.37	-43.58
v_w	2-ODE	1.00	-3.83	1.25	-8.08	17.50	13.27	-33.54
ϕ_u	9-ODE	-1.00	2.67	-0.01	2.40	-9.18	-12.50	31.42
ϕ''_u	2-ODE	-1.00	2.65	-0.01	2.54	-10.37	-10.35	24.50
ϕ_w	9-ODE	1.00	-2.67	0.01	-2.40	9.16	12.50	-31.39
ϕ''_w	2-ODE	1.00	-2.65	0.01	-2.54	10.38	10.35	-24.50

Table 4.3: Local relative sensitivity indices for QOIs (indicated in top labels) with respect to POIs (left columns) for the full model for the 9- and 2-ODE models. The reduced 2-ODE model preserves the order of significance and closely approximates the index values for all the POIs.

5. Discussion and Conclusions. We created and analyzed a hierarchy of reduced models to approximate a detailed system of nine ODEs that describes the spread of *Wolbachia* infection in mosquitoes. Although the original large-scale 9-ODE system captures the detailed transmission dynamics, it would be difficult to analyze the solution if extended to a system of PDEs that includes spatial heterogeneity. We described a procedure to reduce the 9-ODE model to the 7-ODE model by including the impact of the aquatic stage in the adult mosquitoes. We then reduced the 7-ODE model to a two-sex 4-ODE model by accounting for the complex sexual cytoplasmic incompatibility for the pregnant females, without having separate categories for pregnant and nonpregnant females. Finally, we approximated the two-sex 4-ODE model with a single sex 2-ODE model by identifying an approximate relationship between the fraction of infected males and female mosquitoes.

Our step-by-step approach allows us to keep track of the transformations of the parameters at each step of model reduction. As a result, the parameters in the reduced 2-ODE model are defined as the explicit combinations of the ones in the full model. This is essential when applying the model for numerical predictions and giving guidance to the field trials. Without using this approach, it would be very difficult to interpret the biological meanings of the coefficients of the nonlinear terms and, therefore, to estimate their values from the experimental data. The final equations are for the infected and uninfected female mosquito population, which is responsible for the transmission of zoonotic diseases, such as chikungunya, dengue fever, and Zika.

We compare the reduced models to the full baseline model from both qualitative and quantitative aspects. We validate the reduced models by comparing the key properties of the models with the 9-ODE model. The reduced models could analytically

preserve the key dimensionless numbers, including the basic next generation numbers and the basic reproductive number. They also maintain the backward bifurcations of the dynamic system and accurately capture the threshold condition for establishing a stable *Wolbachia* epidemic. The numerical simulations verified that the reduced 2-ODE model has similar transient behavior to the full 9-ODE model between the steady states.

We used sensitivity analysis for model predictions with respect to the 9-ODE model parameters and verify that the ranking for the relative sensitivity indices for the reduced 2-ODE model and original 9-ODE model are the same for the basic reproductive number, the threshold condition, the final prevalence of *Wolbachia* infection, and the speed of growth/clearance in *Wolbachia* infection.

Before these models can be used to guide field studies in releasing *Wolbachia* infected mosquitoes in the wild, we need to be fully aware of the assumptions and limitations of the model. We validated the model reduction assumptions for parameters and initial conditions in situations where the infection transmission and populations changed slowly. In practice, a field trial that only releases a large amount of females mosquitoes may break the balance among different compartments of mosquitoes, and the assumption that assumes a proportional male-female ratio is violated. In such cases, the reduced model will be only trustworthy after the initial transients settle down.

Our reduced 2-ODE model describes the dynamics near the mosquito season when the egg development rate and mating rate are close to the baseline values. Since the reduced 2-ODE model is limited to predict the dynamics in female mosquitoes, it cannot be used to model the impact of mitigation efforts, such as larvicide, on aquatic stage. For example, seasonality such as the fluctuation in temperature and humidity plays an important role in mosquito lifecycle. The more complex models are needed to simulate the mosquito populations over wide variations in aquatic stages, such as the infection surviving a long dry spell, or *Wolbachia* wintering over in the egg stage [16].

Our next focus will be to simulate the dynamics of releasing infected mosquitoes into the wild. If *Wolbachia* infected mosquitoes are released in a small spatial region, then even if it is above the critical threshold in the center of the release area, as the mosquitoes diffuse, it will be below the threshold at the edges of the region. This means that the model must capture the spatial diffusion of the mosquitoes to analyze if the *Wolbachia* infection can be sustained at the edge of the infected region. We are extending our 2-ODE model into a 2-PDE model with spatial dynamics to better capture the local random motion of the mosquitoes (diffusion) and advection (wind).

Appendix A. Sensitiviy analysis for reduced models. The appendix extends the sensitivity analysis in subsection 4.5 to compare the relative sensitivity indices for all the reduced models in Table A.1. The reduced models preserve the order of significance and closely approximate the index values for all the POIs. The maternal transmission rate v_w has the largest impact on all the QOIs except $\mathbb{R}_0$. Aside from v_w, the egg-laying rates (ϕ_*) have the most impact on the speed of establishment or clearance of *Wolbachia* epidemics, and female death rates have the most impact on the final prevalence of *Wolbachia* infection.

Acknowledgments. This research was partially supported by the NSF award 1563531 and the NIH-NIGMS Models of Infectious Disease Agent Study (MIDAS) award U01GM097661. The content is solely the responsibility of the authors and does not necessarily represent the official views of the National Science Foundation or

QOI = $\mathbb{R}_0$					
9-ODE		7-ODE		4/2-ODE	
μ_{fw}	-1.06	μ'_{fw}	-1.04	μ'_{fw}	-1.00
μ_{fu}	1.05	μ'_{fu}	1.04	μ'_{fu}	1.00
v_w	1.00	v_w	1.00	v_w	1.00
ϕ_u	-1.00	ϕ'_u	-1.00	ϕ''_u	-1.00
ϕ_w	1.00	ϕ'_w	1.00	ϕ''_w	1.00
σ	0.01	σ	0.00	σ	0.00

QOI = threshold condition					
9-ODE		7-ODE		4/2-ODE	
v_w	-3.87	v_w	-3.83	v_w	-3.83
ϕ_u	2.67	ϕ'_u	2.65	ϕ''_u	2.65
ϕ_w	-2.67	ϕ'_w	-2.65	ϕ''_w	-2.65
μ_{fw}	2.11	μ'_{fw}	2.03	μ'_{fw}	1.93
μ_{fu}	-2.09	μ'_{fu}	-2.02	μ'_{fu}	-1.93
σ	-0.01	σ	-0.01	σ	0.00

QOI = *Wolbachia* prevalence					
9-ODE		7-ODE		4/2-ODE	
v_w	1.29	v_w	1.25	v_w	1.25
μ_{fw}	-0.06	μ'_{fw}	-0.06	μ'_{fw}	-0.06
μ_{fu}	0.06	μ'_{fu}	0.06	μ'_{fu}	0.06
ϕ_u	-0.01	ϕ'_u	-0.01	ϕ''_u	-0.01
ϕ_w	0.01	ϕ'_w	0.01	ϕ''_w	0.01
σ	0.00	σ	0.00	σ	0.00

QOI = Time 40% $\sim$ 80% infection							
9-ODE		7-ODE		4-ODE		2-ODE	
v_w	-7.62	v_w	-7.85	v_w	-8.10	v_w	-8.08
ϕ_w	-2.40	ϕ'_w	-2.45	ϕ''_w	-2.50	ϕ''_w	-2.54
ϕ_u	2.40	ϕ'_u	2.39	ϕ''_u	2.45	ϕ''_u	2.54
μ_{fu}	-2.11	μ'_{fu}	-2.33	μ'_{fu}	-1.94	μ'_{fu}	-2.20
μ_{fw}	1.52	μ'_{fw}	1.55	μ'_{fw}	1.25	μ'_{fw}	1.19
ψ	-0.22	ψ	0.00	ψ	0.00	ψ	0.00
μ_a	-0.04	μ_a	0.00	μ_a	0.00	μ_a	0.00
σ	-0.04	σ	-0.00	σ	0.00	σ	0.00

QOI = Growth rate at 35% infection							
9-ODE		7-ODE		4-ODE		2-ODE	
v_w	15.59	v_w	17.29	v_w	17.51	v_w	17.50
ϕ_u	-9.18	ϕ'_u	-10.32	ϕ''_w	10.34	ϕ''_w	10.38
ϕ_w	9.16	ϕ'_w	10.25	ϕ''_u	-10.29	ϕ''_u	-10.37
μ_{fu}	7.03	μ'_{fu}	7.83	μ'_{fu}	7.14	μ'_{fu}	7.29
μ_{fw}	-6.47	μ'_{fw}	-7.06	μ'_{fw}	-6.49	μ'_{fw}	-6.27
ψ	0.26	σ	0.06	σ	0.00	σ	0.00
μ_a	0.06	ψ	0.00	ψ	0.00	ψ	0.00
σ	0.05	μ_a	0.00	μ_a	0.00	μ_a	0.00

QOI = Time 25% $\sim$ 10% infection							
9-ODE		7-ODE		4-ODE		2-ODE	
v_w	16.37	v_w	13.58	v_w	13.17	v_w	13.27
ϕ_w	12.50	ϕ'_w	10.58	ϕ''_w	10.32	ϕ''_w	10.35
ϕ_u	-12.50	ϕ'_u	-10.56	ϕ''_u	-10.30	ϕ''_u	-10.35
μ_{fw}	-10.87	μ'_{fw}	-9.32	μ'_{fw}	-8.93	μ'_{fw}	-9.05
μ_{fu}	10.19	μ'_{fu}	8.46	μ'_{fu}	8.05	μ'_{fu}	8.06
ψ	-0.25	σ	0.00	σ	0.00	σ	0.00
σ	0.05	ψ	0.00	ψ	0.00	ψ	0.00
μ_a	-0.04	μ_a	0.00	μ_a	0.00	μ_a	0.00

QOI = Clearance rate at 25% infection							
9-ODE		7-ODE		4-ODE		2-ODE	
v_w	-43.58	v_w	-33.65	v_w	-33.48	v_w	-33.54
ϕ_u	31.42	ϕ'_w	-24.58	ϕ''_w	-24.52	ϕ''_u	24.50
ϕ_w	-31.39	ϕ'_u	24.56	ϕ''_u	24.50	ϕ''_w	-24.50
μ_{fw}	25.65	μ'_{fw}	19.92	μ'_{fw}	19.16	μ'_{fw}	19.25
μ_{fu}	-24.87	μ'_{fu}	-19.07	μ'_{fu}	-18.30	μ'_{fu}	-18.26
ψ	0.21	σ	-0.02	σ	-0.00	σ	-0.00
σ	-0.15	ψ	-0.00	ψ	-0.00	ψ	-0.00
μ_a	0.02	μ_a	-0.00	μ_a	-0.00	μ_a	-0.00

Table A.1: Comparison of local relative sensitivity indices for QOIs (indicated in top row) with respect to POIs (columns) for the full 9-ODE model and reduced models. The reduced models capture the order of significance and closely approximate the index values for all the POIs.

the National Institutes of Health.

REFERENCES

[1] M. T. Aliota, S. A. Peinado, I. D. Velez, and J. E. Osorio, *The wMel strain of Wolbachia reduces transmission of Zika virus by Aedes aegypti*, Sci. Rep., 6 (2016), p. 28792.

[2] N. Chitnis, J. M. Hyman, and J. M. Cushing, *Determining important parameters in the spread of malaria through the sensitivity analysis of a mathematical model*, Bull. Math. Biol., 70 (2008), pp. 1272–1296.

[3] H. L. C. Dutra, M. N. Rocha, F. B. S. Dias, S. B. Mansur, E. P. Caragata, and L. A. Moreira, *Wolbachia blocks currently circulating Zika virus isolates in Brazilian Aedes aegypti mosquitoes*, Cell Host Microbes, 19 (2016), pp. 771–774.

[4] K. Hilgenboecker, P. Hammerstein, P. Schlattmann, A. Telschow, and J. H. Werren, *How many species are infected with Wolbachia?–A statistical analysis of current data*, FEMS Microbiol. Lett., 281 (2008), pp. 215–220.

[5] A. A. Hoffmann, I. Iturbe-Ormaetxe, A. G. Callahan, B. L. Phillips, K. Billington, J. K. Axford, B. Montgomery, A. P. Turley, and S. L. O'Neill, *Stability of the wMel Wolbachia infection following invasion into Aedes aegypti populations*, PLoS Negl. Trop. Dis., 8 (2014), p. e3115.

[6] J. M. Hyman, J. Li, and E. A. Stanley, *Modeling the impact of random screening and contact tracing in reducing the spread of HIV*, Math. Biosci., 181 (2003), pp. 17–54.

[7] J. Koiller, M. Da Silva, M. Souza, C. Codeço, A. Iggidr, and G. Sallet, *Aedes, Wolbachia and dengue*, PhD thesis, Inria Nancy-Grand Est, Villers-lès-Nancy, France, 2014.

[8] C. J. McMeniman, R. V. Lane, B. N. Cass, A. W. Fong, M. Sidhu, Y.-F. Wang, and S. L.

O'neill, *Stable introduction of a life-shortening Wolbachia infection into the mosquito Aedes aegypti*, Science, 323 (2009), pp. 141–144.

[9] C. J. McMeniman and S. L. O'Neill, *A virulent Wolbachia infection decreases the viability of the dengue vector Aedes aegypti during periods of embryonic quiescence*, PLoS Negl. Trop. Dis., 4 (2010), p. 748.

[10] L. A. Moreira, I. Iturbe-Ormaetxe, J. A. Jeffery, G. Lu, A. T. Pyke, L. M. Hedges, B. C. Rocha, S. Hall-Mendelin, A. Day, M. Riegler, L. Hugo, B. K. K.N. Johnson, E. McGraw, A. van den Hurk, P. Ryan, and S.L.O'Neill, *A Wolbachia symbiont in Aedes aegypti limits infection with dengue, Chikungunya, and Plasmodium*, Cell, 139 (2009), pp. 1268–1278.

[11] Z. Qu, L. Xue, and J. M. Hyman, *Modeling the transmission of Wolbachia in mosquitoes for controlling mosquito-borne diseases*, SIAM J. Appl. Math., 78 (2018), pp. 826–852.

[12] H. F. Schoof, *Mating, resting habits and dispersal of Aedes aegypti*, Bull. World Health Organ., 36 (1967), pp. 600–601.

[13] L. M. Styer, S. L. Minnick, A. K. Sun, and T. W. Scott, *Mortality and reproductive dynamics of Aedes aegypti (Diptera: Culicidae) fed human blood*, Vector-borne Zoonotic Dis., 7 (2007), pp. 86–98.

[14] W. Tun-Lin, T. Burkot, and B. Kay, *Effects of temperature and larval diet on development rates and survival of the dengue vector Aedes aegypti in north Queensland, Australia*, Med. Vet. Entomol., 14 (2000), pp. 31–37.

[15] A. F. Van den Hurk, S. Hall-Mendelin, A. T. Pyke, F. D. Frentiu, K. McElroy, A. Day, S. Higgs, and S. L. O'Neill, *Impact of Wolbachia on infection with chikungunya and yellow fever viruses in the mosquito vector Aedes aegypti*, PLoS Negl. Trop. Dis., 6 (2012), p. e1892.

[16] D. Vezzani, S. M. Velázquez, and N. Schweigmann, *Seasonal pattern of abundance of Aedes aegypti (Diptera: Culicidae) in Buenos Aires City, Argentina*, Memórias do Instituto Oswaldo Cruz, 99 (2004), pp. 351–356.

[17] T. Walker, P. Johnson, L. Moreira, I. Iturbe-Ormaetxe, F. Frentiu, C. McMeniman, Y. Leong, Y. Dong, J. Axford, P. Kriesner, et al., *The wMel Wolbachia strain blocks dengue and invades caged Aedes aegypti populations*, Nature, 476 (2011), pp. 450–453.

[18] L. Xue, X. Fang, and J. M. Hyman, *Comparing the effectiveness of different strains of Wolbachia for controlling chikungunya, dengue fever, and Zika*, PLoS Negl. Trop. Dis., 12 (2018), p. e0006666.

[19] L. Xue, C. A. Manore, P. Thongsripong, and J. M. Hyman, *Two-sex mosquito model for the persistence of Wolbachia*, J. Biol. Dyn., (2016), pp. 1–22.

[20] B. Zheng, M. Tang, J. Yu, and J. Qiu, *Wolbachia spreading dynamics in mosquitoes with imperfect maternal transmission*, J. Math. Biol., 76 (2018), pp. 235–263.